Structural, electronic, and magnetic properties of boron cluster anions doped with aluminum: B_nAl^- $(2 \leq n \leq 9)$*

Gu Jian-Bing(顾建兵)[a], Yang Xiang-Dong(杨向东)[a)†], Wang Huai-Qian(王怀谦)[b], and Li Hui-Fang(李慧芳)[a]

[a] *Institute of Atomic and Molecular Physics, Sichuan University, Chengdu* 610065, *China*
[b] *College of Engineering, Huaqiao University, Quanzhou* 362021, *China*

(Received 27 August 2011; revised manuscript received 15 October 2011)

The geometrical structures, relative stabilities, electronic and magnetic properties of small B_nAl^- $(2 \leq n \leq 9)$ clusters are systematically investigated by using the first-principles density functional theory. The results show that the Al atom prefers to reside either on the outer-side or above the surface, but not in the centre of the clusters in all of the most stable B_nAl^- $(2 \leq n \leq 9)$ isomers and the one excess electron is strong enough to modify the geometries of some specific sizes of the neutral clusters. All the results of the analysis for the fragmentation energies, the second-order difference of energies, and the highest occupied-lowest unoccupied molecular orbital energy gaps show that B_4Al^- and B_8Al^- clusters each have a higher relative stability. Especially, the B_8Al^- cluster has the most enhanced chemical stability. Furthermore, both the local magnetic moments and the total magnetic moments display a pronounced odd–even oscillation with the number of boron atoms, and the magnetic effects arise mainly from the boron atoms except for the B_7Al^- and B_9Al^- clusters.

Keywords: boron–aluminum cluster, geometric structure, relative stability, density functional theory

PACS: 31.15.es **DOI:** 10.1088/1674-1056/21/4/043102

1. Introduction

In recent years, an increasing interest in the area of the physical and chemical properties of boron and doped-boron clusters has been aroused due to their potential applications in designing nanoscopic devices and catalysts. Many types of boron clusters have been investigated experimentally and theoretically.[1–9] In light of the experimental data and computational simulations, one can find that the planar or the quasi-planar nuclear arrangement is consistently more stable than any of the other three-dimensional structures for small-sized boron clusters. Besides the studies of pure clusters, many studies of doped clusters containing boron atoms have been conducted.[10–18] For instance, the photoelectron spectra of one or two B atoms doped aluminum clusters $Al_nB_m^-$ ($n \geq 5$ for $m = 1$, $n \geq 10$ for $m = 2$) have been reported,[15] and the mass spectra of $Al_nB_m^-$ ($m + n = 3$–8, $m = 1$–2) clusters have been investigated by Jiang *et al.*[16] In addition, a number of theoretical calculations on Al–B mixed clusters have also been reported.[19–23] For example, Feng and Luo[21] used the density functional theory (DFT) to calculate the structures and stabilities of the Al-doped boron clusters up to $n = 12$. Subsequently, Böyükataa and Güvenc[23] further determined the electronic and the structural properties of AlB_n ($n = 1$–14) with the same method.[23]

Up to now, the have been only a few reports on mixed aluminum boron B_nAl^- clusters. However, interest in their potential applications has spurred considerable activity over the past couple of years. Especially, Romanescu *et al.*[24] recently published the results of experimental photoelectron spectroscopic and computational studies of two Al-doped boron clusters B_6Al^- and $B_{11}Al^-$. Subsequently, the structural and electronic properties of two aluminum-doped boron clusters B_7Al^- and B_8Al^- have been investigated by Galeev *et al.*[25] using photoelectron spectroscopy and *ab initio* calculations. Nevertheless, there has been no systematic theoretical investigation on clusters of B_nAl^- $(2 \leq n \leq 9)$ until now. It is not known whether their structures and properties differ greatly

*Project supported by the National Natural Science Foundation of China (Grant Nos. 10974139 and 10964002) and the Doctoral Program Foundation of the Institution of Higher Education of China (Grant No. 20050610010).

†Corresponding author. E-mail: xdyang@scu.edu.cn

© 2012 Chinese Physical Society and IOP Publishing Ltd

from those of neutral B_nAl clusters. Therefore there is an urgent need to discuss the structural, electronic, and magnetic properties in small boron cluster anions doped with aluminum.

In the present work, we systematically perform a DFT investigation on the stable geometrical structures, relative stabilities, electronic and magnetic properties of aluminum-doped boron B_nAl^- ($2 \leq n \leq 9$) clusters and compare the results with those of the corresponding neutral clusters. All of the structures reported here have positive vibrational frequencies toward the nuclear displacements and therefore correspond to the potential energy minima. Our work is expected to be useful for understanding the influence of the material structure on its properties and so offer relevant information for further experimental and theoretical studies. The rest of the present paper is organized as follows. In Section 2 we give a brief description of the theoretical approach. The geometrical structures, the relative stabilities, the electronic and the magnetic properties of the aluminum-doped boron clusters B_nAl^- ($2 \leq n \leq 9$) are given in Section 3. Conclusions are drawn from the present study in Section 4.

2. Theoretical methods and computational details

The ground states of the B_nAl^- ($2 \leq n \leq 9$) clusters are determined by means of generalized gradient approximation to DFT using GAUSSIAN 03 programs.[26] BPW91, the gradient-corrected Becke's exchange[27] combined with Perdew–Wang's correlation functionals[28] is employed in these calculations. The reliability of the present computational method is validated by calculating the first vertical detachment energy

$$(\mathrm{VDE} = E_{\text{neutral at optimized anion geometry}} - E_{\text{optimized anion}}),$$

for which the experimental results are available.

Table 1. Experimental vertical detachment energies (VDEs) of B_6Al^-, B_7Al^-, and B_8Al^- clusters compared with those calculated for the lowest-energy isomers.

Cluster	B3LYP	BP86	BLYP	BPW91	Expt
B_6Al^-	2.29	2.58	2.24	2.47	2.49
B_7Al^-	3.11	3.21	5.23	3.11	3.31
B_8Al^-	3.80	3.76	3.76	3.57	3.66

The calculated results using the B3LYP,[29−31] BP86,[32] BLYP,[33] and BPW91[27,28] functions are presented in Table 1 and compared with experimental values.[24,25] The results obtained using BPW91 functional[27,28] are the closest to the experimental data, which can be clearly seen from Table 1. Therefore, the BPW91 functional and the 6-311+G(d) basis set can jointly well describe the interactions between the atoms and can be applied to B_nAl^- clusters.

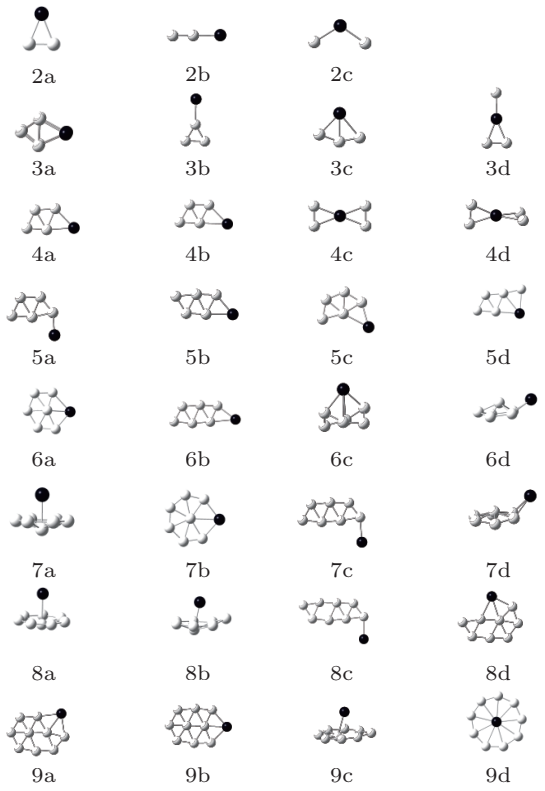


Fig. 1. The lowest-energy structures and low-lying isomers for B_nAl^- ($2 \leq n \leq 9$) clusters, where the black and the gray balls represent Al and B atoms, respectively.

For the optimization process of each cluster geometries, a considerable number of possible initial structures are explored. Here we only list a number of the lowest-energy structures and low-lying isomers in Fig. 1. In addition, all allowable spin multiplicities are considered for a given initial structure: spin-restricted DFT calculations are employed for the singlet state, while spin-unrestricted DFT calculations are employed for all other electronic states. Vibration frequencies are also analysed with the purpose of confirming the stability of structure. If an imaginary vibrational mode is found, a relaxation along the coordinates of the imaginary vibrational mode is carried

out until the true minimum is actually obtained. In addition, the total energies of these lowest-energy clusters determined in our optimizations are then used to study the evolution of their first vertical electron detachment energies, average binding energies, fragmentation energies, and second-order difference of energies each as a function of cluster size. All charge populations are obtained with natural population analysis (NPA),[34,35] and the gaps between the highest occupied molecular orbital (HOMO) and the lowest unoccupied molecular orbital (LUMO) for the most stable isomers are obtained in our optimizations as well.

3. Results and discussion

We determine the optimized geometries of the lowest-energy structures and obtain a number of low-lying isomers for B_nAl^- clusters up to $n = 9$ at DFT/BPW91/6-311+G(d) level, which are described in Section 2. According to the total energy from low to high, the different low-lying isomers are designated by na, nb, nc, and nd, where n is the number of B atoms in B_nAl^- clusters. The lowest-energy structures and some low-lying metastable isomers are presented in Fig. 1. In addition, detailed information about the electronic states, symmetries, lowest frequencies, HOMO and LUMO energies, as well as the natural charge populations (NCP) of Al atoms in the B_nAl^- clusters are listed in Table 2.

Table 2. Electronic states, symmetries, lowest frequencies, HOMO energies, LUMO energies, and natural charge populations (NCP) of Al atoms for B_nAl^- ($2 \leq n \leq 9$) clusters (1 hartree=27.21 eV).

Isomer	State	Symmetry	Frequency/cm^{-1}	HOMO/hartree	LUMO/hartree	NCP of Al/e
2a	$^1A_1$	C_{2v}	501.919	0.006	0.033	0.341
2b	$^3\Sigma$	$C_{\infty v}$	69.027	0.014	0.028	0.247
2c	$^3B_1$	C_{2v}	52.318	0.016	0.029	–0.194
3a	$^2A_1$	C_{2v}	229.030	0.002	0.030	0.411
3b	$^2B_2$	C_{2v}	118.322	0.025	0.034	0.496
3c	$^4A'$	C_s	86.674	0.011	0.020	0.480
3d	$^2B_2$	C_{2v}	107.595	–0.007	0.009	0.456
4a	$^1A'$	C_s	162.132	–0.017	0.033	0.394
4b	$^3A'$	C_s	88.498	0.004	0.001	0.401
4c	$^3A''$	C_{2v}	103.269	–0.030	–0.012	0.755
4d	$^5B_2$	D_{2d}	107.183	–0.022	–0.004	0.706
5a	^2A	C_1	54.363	–0.012	0.015	0.411
5b	^4A	C_1	133.548	–0.012	–0.003	0.541
5c	$^4A''$	C_s	148.356	–0.007	–0.004	0.591
5d	^4A	C_1	181.389	–0.014	0.017	0.633
6a	^1A	C_1	106.799	–0.009	0.024	0.775
6b	^3A	C_1	99.833	–0.036	–0.012	0.538
6c	$^1A'$	C_s	182.710	–0.026	0.044	0.668
6d	^1A	C_1	136.240	–0.022	0.030	0.462
7a	$^2A_1$	C_{6v}	318.101	–0.030	–0.006	0.935
7b	$^2A'$	C_s	51.380	–0.019	0.004	0.849
7c	$^2A'$	C_s	74.464	–0.029	–0.003	0.468
7d	$^2A'$	C_s	95.088	–0.018	0.005	0.585
8a	^1A	C_1	141.695	–0.043	0.080	0.461
8b	$^1A'$	C_s	41.353	–0.000	–0.014	0.966
8c	$^3A'$	C_s	164.035	–0.035	–0.001	0.456
8d	$^3A''$	C_s	143.016	–0.024	0.000	0.733
9a	^2A	C_1	92.436	–0.036	–0.013	0.804
9b	$^2A''$	C_s	85.084	–0.026	0.000	0.853
9c	$^2A'$	C_s	88.999	–0.047	0.012	0.539
9d	$^2A'$	C_s	72.119	–0.001	0.011	1.515

3.1. Equilibrium geometry

The calculated results for BAl^- show that the quartet spin state is 0.28 eV and 2.77 eV lower in energy than the doublet and sextet spin states, respectively. The equilibrium bond distance of BAl^- is calculated to be as long as 2.10 Å (1 Å=0.1 nm), which is longer than that of the BAl (2.05 Å) cluster. Whereas, the calculated bond energy of the BAl^- (3.39 eV) is bigger than that of the BAl (2.24 eV), calculated for the dissociation into B and Al), indicating that the B–Al^- bond is stronger than the B–Al bond and the one excess electron can strengthen the stability of BAl.

All possible initial structures of the B_2Al^- cluster, i.e., linear structures ($D_{\infty h}$, $C_{\infty v}$) as well as the triangle structures (acute angle or obtuse angle), are optimized at the BPW91 level. Calculated results show that the lowest-energy isomer 2a (Fig. 1), is an isosceles triangle structure (C_{2v}), with two B–Al bonds of 2.05 Å and one B–B bond of 1.54 Å. The energetically closest isomer 2b is a triplet state ($^3\Sigma$) with $C_{\infty v}$ symmetry, which is 0.90 eV higher in energy than 2a. Moreover, the obtuse isosceles triangle structure, isomer 2c, with an apex angle of 113.54° is the least stable structure of B_2Al^- cluster in Fig. 1. It should be pointed out that isomers 2a and 2b also occur in the case of the neutral B_2Al cluster,[23] while the isomer 2c is not confirmed as local minima in the B_2Al cluster optimizations.[23]

In the case of $n = 3$, the lowest-energy isomer 3a (shown in Fig. 1) can be obtained by adding one boron atom directly to the most stable structure 2a of B_2Al^- cluster and the structure of isomer 3a is the third isomer in the B_3Al cluster optimizations.[23] The second stable structure 3b for B_3Al^- is a Y-shaped structure with the symmetry of C_{2v} and the electronic state of $^2B_2$, and it is the ground-state structure for a neutral B_3Al cluster. Isomer 3c is found within an energy range of 1.33 eV, and it has a shape of plane C_s rhombus with a quartet electronic state ($^4A'$). From Fig. 1, we can clearly see that the isomer 3d is also a Y-like structure, which is similar to the structure of the isomer 3b. Whereas, the Al atoms are at the different positions in both structures of 3b and 3c. Besides, the calculated VDE value of the ground-state structure 3a is 2.47 eV.

With respect to B_4Al^- cluster, both the lowest-energy structure 4a and the energetically closest isomer 4b (see Fig. 1) are consistent with the equivalent of the neutral B_4Al cluster,[23] which can be obtained by capping one boron atom on the peripheral site of the most stable B_3Al^- frame with a little distortion. The VDE value (2.67 eV) for the ground-state structure 4a is achieved in our calculations. Isomer 4b is 0.77 eV higher in energy than the ground-state structure 4a. Moreover, by adding one boron atom directly into the structure of the isomer 3d, the planner X-like structure 4c and three-dimensional (3D) X-like structure 4d can be created. Surprisingly, isomer 4c has a relatively high symmetry of D_{2d}.

As for the B_5Al^- cluster, numerous possible initial geometries are optimized. According to the calculated results, it should be pointed out that the lowest-energy structure is also a planar configuration, which is consistent with the result of the neutral B_5Al cluster.[21] As shown in Fig. 1, the ground-state structure 5a with the electronic state of ^2A can be regarded as a stable B_5 frame[6] with one Al atom capped on the peripheral position with a little distortion and its first VDE value (2.63 eV) is also obtained in our theoretical calculations. The energy closest to isomer 5b can be viewed as the overlap of two rhombus structures, which is only 0.16 eV less stable than the 5a isomer. The planar 5c isomer, in the electronic state of $^4A''$, is 0.38 eV higher in energy than the ground-state 5a. Furthermore, we also find the least stable structure 5d within an energy range of 0.76 eV, which can be regarded as a deformed trapezoid built up by six atoms.

In the optimization process, four different isomers (6a, 6b, 6c, and 6d) within an energy range of 0.25 eV are found. The lowest-energy hexagon-shaped isomer 6a is a quasi-planar structure with the symmetry of C_s and the electronic state of $^1A'$. Its calculated VDE value is 2.47 eV, which is in good agreement with the experimental result (2.49±0.03 eV).[24] The planar trapezoidal structure 6b, composed of seven atoms, is the second-stable structure with respect to the isomer 6a. In addition, the other two low-lying isomers 6c and 6d (shown in Fig. 1) with low symmetry are also found for B_6Al^- cluster and their energies are 0.22 eV and 0.25 eV higher than those of the ground state respectively. It is worthwhile pointing out that all the results obtained in our calculations are in excellent agreement with the results given by Romanescu *et al.*[24]

For $n = 7$, the umbrella-type isomer 7a (C_{6v},$^2A_1$), which is similar to the structure of the B_7Li^-[18] and consistent with the previous result,[25] is the ground-state structure of B_7Al^- cluster. Its VDE value

(3.11 eV) is also obtained in our theoretical calculations, which is somewhat lower than the experimental result (3.31 eV).[25] The planar structure 7b, a deformed heptagon with a boron atom in the centre, is the lowest-energy structure in the case of the neutral B_7Al cluster optimizations.[23] The appreciable geometry change from B_7Al to B_7Al^- is caused by the one excess electron. Again, we perform an extensive search for other low-lying isomers. The following structures 7c and 7d are 0.80 eV and 0.81 eV higher in energy than the isomer 7a, respectively.

As for $n = 8$, four stable structures denoted as 8a, 8b, 8c, and 8d, are optimized to be the minima at the energy surface. As shown in Fig. 1, the umbrella-type isomer 8a, which can be obtained by adding one Al atom above the 7-boron ring plane, is the lowest-energy structure. This geometry is not only consistent with the previous result[25] but also similar to the ground-state structure of the neutral B_8Al cluster.[23] On the basis of the optimized structure (8a), the single-point energy of the neutral isomer with the same anion geometry is calculated, so the corresponding VDE value (3.57 eV) is obtained, which is somewhat smaller than the experimental result (3.66 eV). Isomer 8b, with the symmetry of C_s and electronic state of $^3A'$, is the second stable structure in comparison with isomer 8a. In addition, isomers 8c and 8d, which possess identical structural symmetry (C_s) and different electronic states ($^1A'$ for 8c and $^3A''$ for 8d), are also obtained in our optimization process.

For B_9Al^- clusters shown in Fig. 1, the dovetailed hexagonal bipyramid structure 9a, which corresponds to the second-stable isomer in the case of the B_9Al cluster optimizations,[23] is the most stable structure of B_9Al^- cluster and its calculated VDE value is 3.08 eV. The second stable isomer 9b and the umbrella-like structure 9c are also obtained in the energy range of 0.65 eV. The planar wheel structure 9d is only an isomer fully constructed boron ring around the Al atom. Though the isomer 9b in a high coordinated position, it does not correspond to the lowest-energy and it is 0.83 eV higher in energy than the isomer 9a so it is less stable than the isomer 9a. However, this geometry is the ground-state structure in the neutral B_9Al cluster optimizations.[23]

According to the above discussion, the ground-state isomers for B_nAl^- ($2 \le n \le 9$) are different from those of the corresponding neutral B_nAl clusters except B_2Al^-, B_6Al^-, and B_8Al^-. This indicates that the one excess electron is strong enough to modify the geometries of some specified sizes of neutral clusters. Moreover, it is worthwhile pointing out that the Al atom prefers to reside either on the outer side or above the surface, not in the centre in all of the most stable B_nAl^- ($2 \le n \le 9$) structures.

In light of the calculated VDE values, we plot each of them as a function of cluster size in Fig. 2. From the figure, two local peaks occurring at $n = 4$ and $n = 8$ can be clearly observed. Unfortunately, there have been no experimental data of VDE for B_nAl^- ($2 \le n \le 9$) clusters except B_6Al^-, B_7Al^-, and B_8Al^- clusters until now. Therefore, it is expected that our theoretical results will provide some guidance for further experiments aiming at determining the VDE values of B_nAl^- ($2 \le n \le 9$) clusters.

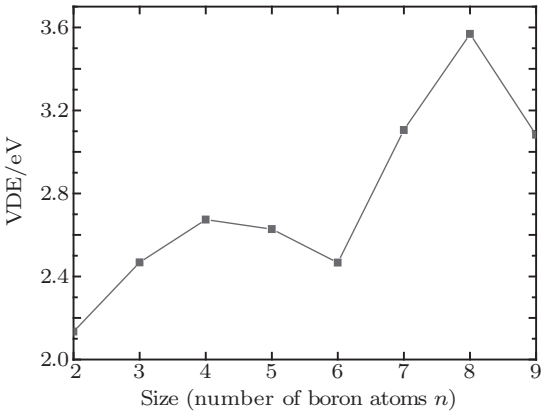


Fig. 2. Size dependence of the calculated vertical electron detachment energies (VDE) for the lowest-energy structures of B_nAl^- ($2 \le n \le 9$) clusters.

3.2. Relative stability

In order to predict the relative stabilities of B_nAl^- ($2 \le n \le 9$) clusters, we calculate the values of average binding energy E_b, fragmentation energy $\Delta_1 E$, and second-order difference of the total energy $\Delta_2 E$ for isomers with the lowest-energies by using the following formulas:

$$E_b(B_nAl^-) = \frac{E(Al^-) + nE(B) - E(B_nAl^-)}{n+1}, \quad (1)$$

$$\Delta_1 E(B_nAl^-) = E(B_{n-1}Al^-) + E(B) - E(B_nAl^-), \quad (2)$$

$$\Delta_2 E(B_nAl^-) = E(B_{n-1}Al^-) + E(B_{n+1}Al^-) - 2E(B_nAl^-), \quad (3)$$

where $E(Al^-)$, $E(B)$, $E(B_nAl^-)$, $E(B_{n-1}Al^-)$, and $E(B_{n+1}Al^-)$ respectively represent the total energies of the most stable Al^-, B, B_nAl^-, $B_{n-1}Al^-$, and $B_{n+1}Al^-$ clusters. In addition, for B_nAl^- clusters the

calculated values of average binding energy E_b, fragmentation energy $\Delta_1 E$, and the second-order difference of the total energy $\Delta_2 E$ are plotted as curves in Figs. 3(a), 3(b), and 3(c), respectively. As presented in Fig. 3(a), the average binding energies of B_nAl^- and B_nAl clusters both increase monotonically with cluster size, which reflects the fact that the bigger the cluster, the more stable the molecular property is. Meanwhile, that the average binding energies of B_nAl clusters are smaller than those of B_nAl^- clusters can also be clearly seen from Fig. 3(a), implying that the one excess electron can improve the stability of neutral B_nAl clusters. Furthermore, there are two visible peaks in the curve, located at $n = 4$ and 8, indicating that B_4Al^- and B_8Al^- clusters are more stable than their neighbouring clusters.

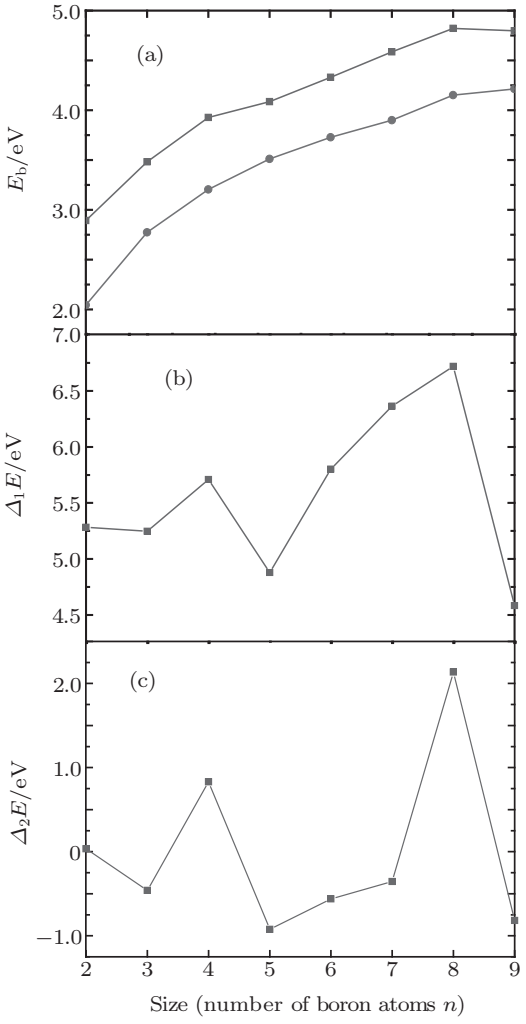


Fig. 3. (a) Average binding energies for the lowest-energy structures of B_nAl^- (solid squares) and B_nAl (solid dots Ref. [23]) each as a function of cluster size. Size dependence of the fragmentation energies (b), and the second-order difference energies (c) for the lowest-energy structures of B_nAl^- clusters.

In cluster physics, the fragmentation energies and second-order difference of energies are sensitive quantities that reflect the relative stabilities. Therefore, the size dependences of the fragmentation energies and second-order difference of energies for B_nAl^- ($2 \le n \le 9$) clusters are further investigated. As presented in Figs. 3(b) and 3(c), the local peaks located at $n = 4$ and 8 in both curves of the fragmentation energies and second-order difference of energies imply that B_4Al^- and B_8Al^- clusters keep high stability compared with the clusters in their vicinity. These are consistent with the calculated results of the average binding energies. Furthermore, as shown in Fig. 3(a)–3(c), the maximum magic number of the relative stability is $n = 8$ among the investigated B_nAl^- ($2 \le n \le 9$) clusters, reflecting that the B_8Al^- cluster is the most stable geometry, which is in good agreement with the calculated VDE result.

3.3. Electronic properties

The electronic properties of B_nAl^- clusters are discussed by examining the energy gap between the HOMO and the LUMO, because the HOMO–LUMO energy gap reflects the ability for electrons to jump from an occupied orbital to an unoccupied orbital and can also provide an important criterion for judging the chemical stability of clusters to some degree. A large gap corresponds to a high strength required to perturb the electronic structure. In general, a bigger gap indicates a weaker chemical activity, while a smaller one corresponds to a stronger chemical activity. Furthermore, the HOMO and LUMO energies for the lowest-energy and low-lying isomers of B_nAl^- clusters are summarized in Table 2. Meanwhile, the size dependence of HOMO–LUMO gaps for the ground-state isomers of B_nAl^- is plotted in Fig. 4. For comparison, the size dependence of HOMO–LUMO gaps for the lowest-energy B_nAl structures is also plotted in Fig. 4.

As seen from Fig. 4, the primary features are concluded as follows. (i) The HOMO–LUMO energy gaps for the most stable B_nAl^- ($2 \le n \le 9$) clusters range from 0.63 eV to 3.35 eV. (ii) It is interesting to note that the HOMO–LUMO gaps exhibit bigger oscillations at $n = 4$ and 8, indicating that B_4Al^- and B_8Al^- clusters are more stable than their neighbouring clusters, which is in accordance with the behaviours of the fragmentation energies and second-order difference of energies versus n (Figs. 3(b) and

3(c)). (iii) In particular, the cluster of B_8Al^- has a largest HOMO–LUMO gap of 3.35 eV, implying that B_8Al^- cluster has dramatically enhanced chemical stability and can be viewed as building block for constructing the cluster-assembled materials. (iv) It should also be pointed out that the variation trend of the HOMO–LUMO energy gaps for B_nAl^- clusters is consistent with that for the neutral B_nAl clusters.

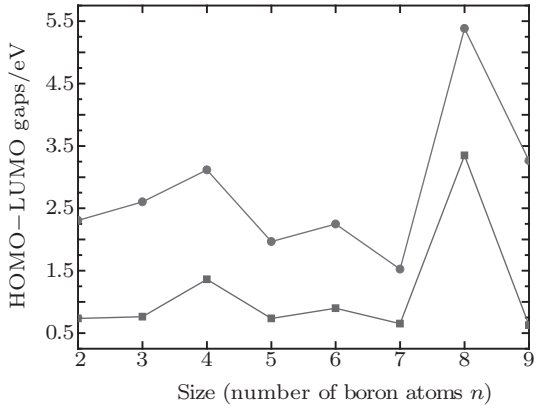


Fig. 4. Size dependences of the highest occupied-lowest unoccupied molecular orbital energy gaps for the lowest-energy structures of B_nAl^- (solid squares) and B_nAl (solid dots Ref. [23]) clusters.

For giving a reasonable explanation of the charge transfer within the clusters, the natural population analysis (NPA) has been performed in this part, and the NPA results of the Al atom for the lowest and low-lying energy B_nAl^- species are summarized in Table 2. From Table 2, we can clearly see that the charge tends to transfer from Al atom to B atom and the charge transfers are in a range of 0.34–0.94 electrons in the ground-state B_nAl^- ($2 \leq n \leq 9$) structures. That is, the Al atom behaves as an electron donor in all stable B_nAl^- ($2 \leq n \leq 9$) clusters. This phenomenon may be caused by a difference in electronegativity between Al (1.61) and B (2.05).

3.4. Magnetic properties

On the basis of the most stable geometries, the total magnetic moments of B_nAl^- ($2 \leq n \leq 9$) as well as the local magnetic moments of Al atoms in B_nAl^- clusters are presented in Fig. 5. As seen from Fig. 5, each of the total magnetic moments of the most stable B_nAl^- clusters as a function of cluster size shows a dramatic odd–even alternative behaviour. For the B_nAl^- clusters with even-number boron atoms, the total magnetic moment is zero, whereas for odd n, the value is 1 μ_B. In addition, the total magnetic moment is located mainly on the B atoms except for B_7Al^- and B_9Al^-, whereas the magnetic moment located at the Al atoms is small (about 0.05 μ_B–0.45 μ_B).

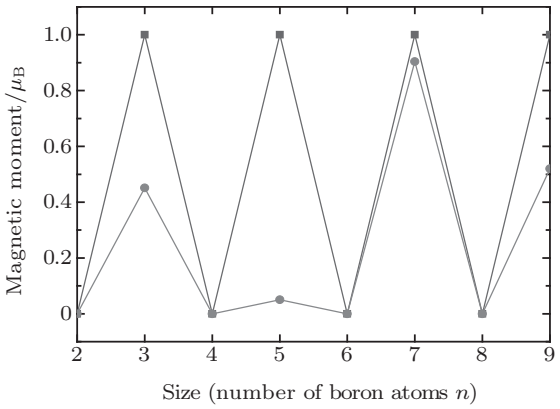


Fig. 5. Size dependences of the total magnetic moments of the B_nAl^- clusters (solid squares), and the local magnetic moments on the Al atoms (solid dots).

To better understand the magnetic properties of B_nAl^- ($2 \leq n \leq 9$) clusters, we perform a detailed analysis of the local magnetic moments of Al atom in the lowest-energy B_nAl^- clusters. The local magnetic moments of 3s, 3p, and 3d states for the Al atoms are summarized in Table 3. As shown in Table 3, the magnetic moment of the Al atom is mainly from the 3p state except for the B_7Al^- cluster, the next is the 3s state, and the 3d state has no contribution to the magnetic moment of the Al atom.

Table 3. Values of total magnetic moment (μ_t) of B_nAl^- clusters, local magnetic moment (μ_{Al}) of Al atom, and magnetic moment of 3s, 3p, and 3d states for Al atom in the lowest-energy B_nAl^- ($2 \leq n \leq 9$) clusters.

Cluster	μ_t	μ_{Al}	3s	3p	3d
B_2Al^-	0	0	0.00	0.00	0.00
B_3Al^-	1	0.45	0.13	0.32	0.00
B_4Al^-	0	0	0.00	0.00	0.00
B_5Al^-	1	0.05	0.01	0.04	0.00
B_6Al^-	0	0	0.00	0.00	0.00
B_7Al^-	1	0.90	0.46	0.44	0.00
B_8Al^-	0	0	0.00	0.00	0.00
B_9Al^-	1	0.52	0.22	0.29	0.00

4. Conclusion

The geometrical structures, the relative stabilities, the electronic and the magnetic properties of different sized Al-doped boron B_nAl^- ($2 \leq n \leq 9$) clusters are investigated systematically by employing the density functional calculations at the BPW91 level

with the basis set of 6-311+G(d). The main results are summarized in the following.

(I) All of the ground-state isomers of B_nAl^- ($2 \leq n \leq 9$) clusters are different from the corresponding neutral B_nAl clusters except B_2Al^-, B_6Al^-, B_8Al^- and the Al atom prefers to reside either on the outer side or above the surface, but not in the centre of the clusters.

(II) The size dependences of the fragmentation energies, second-order difference of energies, and the HOMO–LUMO energy gaps of the lowest-energy structures are discussed separately. It is worthwhile pointing out that the clusters of B_4Al^- and B_8Al^- have higher stability than their neighbouring clusters. Especially, the B_8Al^- cluster shows the strongest stability due to its maximum peak in all of the curves (Figs. 3(b), 3(c), and Fig. 4). In addition, the one excess electron is strong enough to modify the geometries of some specific sizes of neutral clusters and can improve the stabilities of the corresponding neutral clusters.

(III) As for the influence of the cluster size on magnetic moment, a pronounced odd–even oscillatory phenomenon is observed separately for the local magnetic moment of the Al atom and for the total magnetic moments of B_nAl^- clusters. Namely, the lowest-energy structures of B_nAl^- ($2 \leq n \leq 9$) clusters with odd-numbered boron atoms each have a total magnetic moment of 1 μ_B, which is located mainly on the boron atoms, whereas for even-numbered boron atoms they exhibit nonmagnetic ground states.

References

[1] Zhai H J, Wang L S, Alexandrova A N, Boldyrev A I and Zakrzewski V G 2003 *J. Phys. Chem.* A **107** 9319

[2] Zhai H J, Kiran B, Li J and Wang L S 2003 *Nat. Mater.* **2** 827

[3] Zhai H J, Wang L S, Alexandrova A N and Boldyrev A I 2003 *Angew. Chem. Int. Ed.* **42** 6006

[4] Alexandrova A N, Boldyrev A I, Zhai H J and Wang L S 2004 *J. Phys. Chem.* A **108** 3509

[5] Alexandrova A N, Boldyrev A I, Zhai H J, Wang L S, Sheiner E and Fowler P 2003 *J. Phys. Chem.* A **107** 1359

[6] Zhai H J, Wang L S, Alexandrova A N and Boldyrev A I 2002 *J. Chem. Phys.* **117** 7917

[7] Boustani I 1997 *Phys. Rev.* B **55** 16426

[8] Lau K C, Deshpande M, Patt R and Pandey R 2005 *Int. J. Quantum Chem.* **103** 866

[9] Liu L R, Lei X L, Chen H and Zhu H J 2009 *Acta Phys. Sin.* **58** 5355 (in Chinese)

[10] Liu Z F, Lei X L, Liu L R, Liu H Y and Zhu H J 2011 *Chin. Phys.* B **20** 023101

[11] Lei X L, Zhu H J, Ge G X, Wang X M and Luo Y H 2008 *Acta Phys. Sin.* **57** 5491 (in Chinese)

[12] Lei X L, Wang Q L, Yan Y L, Zhao W J, Yang Z and Luo Y H 2007 *Acta Phys. Sin.* **56** 4484 (in Chinese)

[13] Yang Z, Yan Y L, Zhao W J, Lei X L, Ge G X and Luo Y H 2007 *Acta Phys. Sin.* **56** 2590 (in Chinese)

[14] Chen Y H, Zhang C R and Ma J 2006 *Acta Phys. Sin.* **55** 171 (in Chinese)

[15] Kawamata H, Negishi Y, Nakajima A and Kaya K 2001 *Chem. Phys. Lett.* **337** 255

[16] Jiang Z Y, Luo X M, Li S T and Chu S Y 2006 *Int. J. Mass Spectrom.* **252** 197

[17] Lei X L 2011 *J. Clust. Sci.* **22** 159

[18] Tai T B and Nguyen M T 2010 *Chem. Phys.* **375** 35

[19] Averkiev B B and Boldyrev A I 2008 *Russ. J. Gen. Chem.* **78** 769

[20] Averkiev B B, Wang L M, Huang W, Wang L S and Boldyrev A I 2009 *Phys. Chem. Chem. Phys.* **11** 9840

[21] Feng X J and Luo Y H 2007 *J. Phys. Chem.* A **111** 2420

[22] Guo J C, Yao W Z, Li Z and Li S D 2009 *Sci. China* Ser. B: *Chem.* **52** 566

[23] Böyükataa M and Güvenc Z B 2011 *J. Alloys Compd.* **509** 4214

[24] Romanescu C, Sergeeva A P, Li W L, Boldyrev A I and Wang L S 2011 *J. Am. Chem. Soc.* **133** 8646

[25] Galeev T R, Romanescu C, Li W L, Wang L S and Boldyrev A I 2011 *J. Chem. Phys.* **135** 104301

[26] Frisch M J, Trucks G W, Schlegel H B, Scuseria G E, Robb M A, Cheeseman J R, Montgomery J A, Vreven T, Kudin K N, Burant J C, Millam J M, Iyengar S S, Tomasi J, Barone V, Mennucci B, Cossi M, Scalmani G, Rega N, Petersson G A, Nakatsuji H, Hada M, Ehara M, Toyota K, Fukuda R, Hasegawa J, Ishida M, Nakajima T, Honda Y, Kitao O, Nakai H, Klene M, Li X, Knox J E, Hratchian H P, Cross J B, Adamo C, Jaramillo J, Gomperts R, Stratmann R E, Yazyev O, Austin A J, Cammi R, Pomelli C, Ochterski J W, Ayala P Y, Morokuma K, Voth G A, Salvador P, Dannenberg J J, Zakrzewski V G, Dapprich S, Daniels A D, Strain M C, Farkas O, Malick D K, Rabuck A D, Raghavachari K, Foresman J B, Ortiz J V, Cui Q, Baboul A G, Clifford S, Cioslowski J, Stefanov B B, Liu G, Liashenko A, Piskorz P, Komaromi I, Martin R L, Fox D J, Keith T, Al-Laham M A, Peng C Y, Nanayakkara A, Challacombe M, Gill P M W, Johnson B, Chen W, Wong M W, Gonzalez C and Pople J A 2004 *Gaussian* 03 Revision E.01 (Wallingford CT: Gaussian, Inc.)

[27] Becke A D 1988 *Phys. Rev.* A **38** 3098

[28] Perdew J P and Wang Y 1992 *Phys. Rev.* B **45** 13244

[29] Becke A D 1993 *J. Chem. Phys.* **98** 5648

[30] Lee C, Yang W and Parr R G 1988 *Phys. Rev.* B **37** 785

[31] Mielich B, Savin A, Stoll H and Preuss H 1989 *Chem. Phys. Lett.* **157** 200

[32] Perdew J P 1986 *Phys. Rev.* B **34** 7406

[33] Lee C, Yang W and Parr R G 1993 *Phys. Rev.* B **37** 785

[34] Reed A E, Curtiss L A and Weinhold F 1985 *J. Chem. Phys.* **83** 735

[35] Reed A E, Curtiss L A and Weinhold F 1988 *Chem. Rev.* **88** 899